

CONTROL OF STREAKY DISTURBANCES IN THE BOUNDARY LAYER OVER A FLAT PLATE

Pierluigi Morra*, Kenzo Sasaki**, André Cavalieri**, Ardeshir Hanifi* & Dan Henningson*

*KTH Royal Institute of Technology, Stockholm, SE-100-44, Sweden

**Instituto Tecnológico de Aeronáutica, São José dos Campos, SP, 12228-900, Brazil

Keywords: *Flow control, streaks, adaptive control, feedforward control.*

Abstract

The present work considers control of perturbations in the boundary layer over a flat plate by means of adaptive methods. In particular, we focus our attention on a control law based on a multi-input-multi-output (MIMO) filtered- x least-mean-square (fxLMS) adaptive algorithm. The studies are performed through direct numerical simulations. The perturbation field studied here mimics those generated by freestream turbulence with different amplitude and scales. Plasma actuators and shear-stress sensors are considered to mimic a real case scenario.

1 Introduction

Since the laminar flow state is characterized by a smaller friction drag than the turbulent one, avoiding or delaying the laminar-to-turbulent transition will reduce the overall drag and contribute to lower energy and fuel consumption required for operating transportation means, such as trains and aircraft. The transition to turbulence of a laminar boundary-layer flows is usually due to growth and breakdown of initially small perturbations. Thus, aiming for damping their growth can be an efficient method to avoid or delay transition to turbulence, and that is the idea behind the present work. The action on the flow can be designed by means of different control techniques, and in the present work we focus on a control law based on a multi-input-multi-output (MIMO) *filtered- x least-mean-square* (fxLMS)

algorithm, which is linear and adaptive [1]. The linearity of the algorithm highly simplifies its design, but at the same time guarantees an almost-persistent off-design working condition, which is the reason for the choice of an adaptive algorithm. Such better off-design performance of the fxLMS algorithm was assessed in the case of TS-waves instabilities [2], where extensive numerical and experimental robustness studies showed positive results. Here, we consider more complex perturbation fields, dominated by streaky structures generated by free-stream turbulence. An example of such condition is the flow over turbine blades.

2 Control strategy

Here, we assume the control action is performed by a row of localized and evenly spaced actuators that force the flow in the proximity of the wall. The actuators are modeled by a forcing field, whose size and strength are varied. Specially, force fields corresponding to plasma actuators are investigated. The computation of the action $u_l(t)$ is based on the measurements $y_m(t)$, which come from a row of sensors placed upstream the actuators, through a kernel function computed on-line and based on the measurements $z_m(t)$, which come from a row of sensors placed downstream the actuators (see Fig. 1). The computation of the kernel function is based on the minimization of a quadratic cost function $J(t)$, with the aim of minimizing the $z_m(t)$ oscillations around a given value; in other terms, it aims at minimizing the

streamwise velocity oscillations around the laminar boundary layer flow. In particular, it reads

$$u_l(t) = \sum_m \int_{t_0}^t K_m(\tau) y_{m+l}(t-\tau) d\tau \quad \forall l, \quad (1)$$

and

$$J(t) := \sum_l z_l^2(t). \quad (2)$$

In eq. (3) we assumed that the kernel function K does not have any dependence on the spanwise position of the actuator. In fact, the most general description of the actuation-sensors relationship would require each actuator depend on the upstream sensors in a unique way, so one should have as many sets of K_m functions as the number of actuators, and the indexing could be K_m^l . In our case, though, the baseflow is homogeneous in the spanwise direction, so we can assume that there is only one set of kernel functions to be used for all actuators; thus, the indexing K_m . In our set-up the number of sensors is equal to the number of actuators and they are placed along straight lines parallel to the spanwise direction (z -direction). Then, assuming to have M upstream sensors y_m and M actuators u_l , the number of transfer functions is reduced from M^2 to M , which decreases substantially the required computational power. The kernel functions K_m are computed on-line by the compensator, which is designed dynamically by means of a MIMO version of the fxLMS algorithm introduced by [3]. The minimization of the cost function (2) requires expressing the measurements z as a function of K . The chosen function is linear, and reads

$$\begin{aligned} z_r(t) &= \sum_l \int_{t_0}^t P_l^{zu}(s) u_{l+r}(t-s) ds \quad \forall r, \\ &= \sum_l \int_{t_0}^t P_l^{zu}(s) \sum_m \int_{s_0}^{t-s} K_m(\tau) y_{m+l}(t-s-\tau) d\tau ds \\ &\quad \forall r, \end{aligned} \quad (3)$$

where P^{zu} is the transfer function from the actuators to the downstream sensors, and needs to be modeled. We do that by collecting the impulse response from the actuators to the downstream sensors. Moreover, the linear system we want

to control is stable, so the kernel functions tend to zero as the dummy time variable τ , $s \rightarrow \infty$. Then, we can choose $t_0 = t - T$ and $s_0 = t - s - S$ and say that for larger values of T or S the kernel functions are so small that their contribution to the integral is negligible. Under this assumption the order of integration can be switched after a time of at least $T + S$ and one can write

$$z_r(t) = \sum_m \int_{t_0}^t K_m(\tau) f_{m+r}(t-\tau) d\tau \quad \forall r, \quad (4)$$

where

$$f_r(t) := \sum_l \int_{t_0}^t P_l^{zu}(\tau) y_{r+l}(t-\tau) d\tau \quad \forall r. \quad (5)$$

The linearity of the model also implies that the signal of the objective $z_l(t)$ is given as a linear combination of the signal given by the disturbance only and the signal given by the actuation only, that is,

$$z_l(t) = z_l(t)_d + z_l(t)_u, \quad (6)$$

which is useful in the minimization of the objective function J . We wish to find the K_m that minimizes J , which can be obtained by computing the gradient

$$\frac{\partial(J(t))}{\partial K_m(\tau)} = 2 \sum_l z_l(t) \frac{\partial z_l(t)}{\partial K_m(\tau)}, \quad (7)$$

and since the only part of z_l that depends on K_m is related to the actuator, one gets

$$\frac{\partial z_l(t)}{\partial K_m(\tau)} = \frac{\partial z_l(t)_u}{\partial K_m(\tau)}. \quad (8)$$

The kernel function K_m is then obtained online by gradient-descent, where the descent direction is given by the gradient of the objective function J with respect to K_m . This is what makes the algorithm adaptive.

3 Sensors and actuators

In the simulation sensing is performed by means of modeled shear-stress sensors, which measure the average $\partial u'_x / \partial y$ (u'_x is the perturbation part of

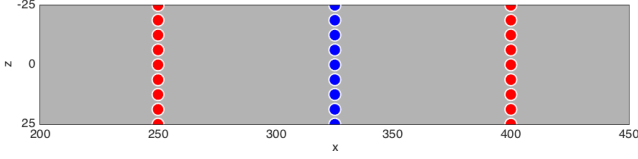


Fig. 1 Sensors and actuators positions; example with 8 devices along the spanwise direction. y_l at $x = 250$; u_l at $x = 325$, z_l at $x = 400$.

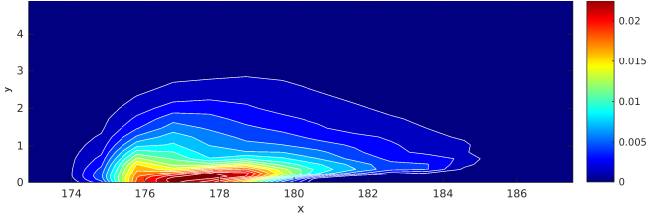


Fig. 2 Plasma actuator. Streamwise component. Bidimensional values from [4].

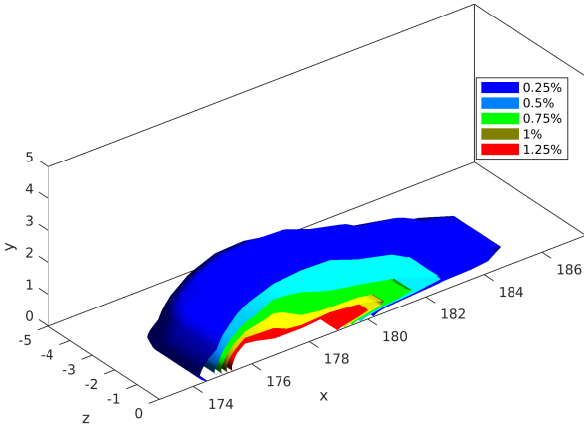


Fig. 3 Plasma actuator. Streamwise component. Three-dimensional isosurfaces.

the streamwise component of the velocity vector) over an area on the wall of the box, that is at $y = 0$, whereas actuation is performed by modeled plasma actuators, which introduce a body force in the Navier-Stokes equations.

Measurements y and z from the flow-field are given by

$$y(t) := \frac{1}{S} \int_S \frac{\partial u'_x}{\partial y} dS, \quad (9)$$

where S is the area over which the velocity gradient is averaged. The z measurement has the same definition.

The actuation signal $u(t)$ is fed into the flow field by multiplication to a body force $\mathbf{b}u(t)$, which is fed into the Navier-Stokes equation. The body force \mathbf{b} represents the actuator itself and need to be modeled to have a spatial shape. The modeling was based on the experimental results by [4] (Fig. 2), which was valid for a two-dimensional profile, so we extruded the shape in the third dimension and multiplied it by a gaussian to avoid discontinuities in that direction (Fig. 3). The body force is applied along the streamwise direction, thus it has the form

$$\mathbf{b} := \{b_x, b_y, b_z\} = \{b_x, 0, 0\}. \quad (10)$$

Sensors and actuators are modeled such that they do not overlap each others in the physical space.

4 Flow case and results

We consider the flow over a flat plate at zero pressure gradient. A perturbation field is imposed at the inflow boundary of the computational domain that mimics the free-stream turbulence. This is done by adding a prescribed number of modes of the continuous spectrum of the linearized Orr-Sommerfeld and Squire operators following the procedure given in [5]. The field is forced to match a prescribed field of the form

$$\mathbf{u}_p = \sum A_N \hat{\mathbf{u}}_N(y) e^{i\beta z + i\text{Re}\{\alpha(\omega, \gamma, \beta)\}x - i\omega t}. \quad (11)$$

An example of the resulting perturbation field is shown in Fig. 4, showing that disturbances develop into streaks.. Computations are for the lin-

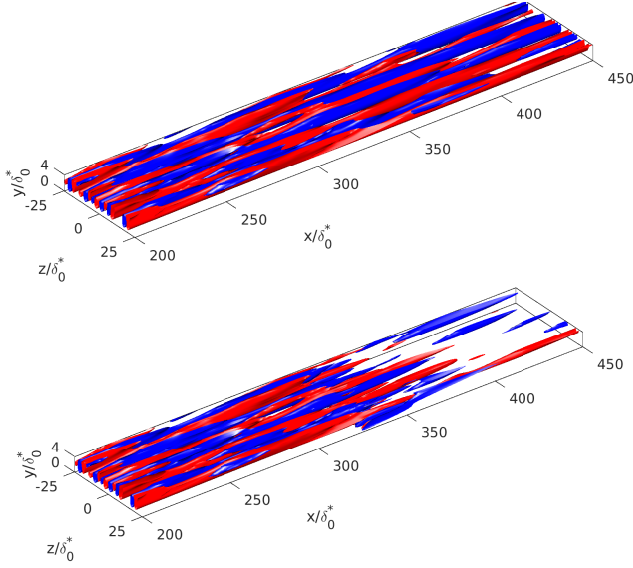


Fig. 4 Isosurface of streamwise perturbation velocity for uncontrolled case (above) and controlled by plasma actuators (below).

earized Navier-Stokes equations only,

$$\frac{\partial \mathbf{u}'}{\partial t} = \mathbf{L}(\mathbf{U}_B) \mathbf{u}' + \mathbf{b}, \quad (12)$$

where \mathbf{L} is a linear operator (namely, the Jacobian resulting from the linearization) dependent on \mathbf{U}_B , which is the Blasius solution around which the linearization is performed, and \mathbf{u}' is the perturbation part of the velocity, and \mathbf{b} a body force. The streamwise extent of the computational domain corresponds to $Re_x \in [0.3, 3.0] \times 10^5$, where $Re_x = xU_\infty/\nu$ is the local Reynolds number. The simulations are performed using SIMSON [6], an efficient pseudo-spectral code.

The performance of the control law can be inspected from two point of views: the behavior of the flow field and the behavior of the signals. This is crucial because the only information reaching the control law is the one carried in the signals, which could be missing some non-negligible feature of the flow field dynamics. In Fig. 4 a snapshot of the uncontrolled and controlled flow fields is shown, and an effective damping of the streaky disturbances at $x = 400$ due to the addition of a counter disturbance at $x = 325$ by means of the actuators appears. The signal behavior shows similar results. The cost

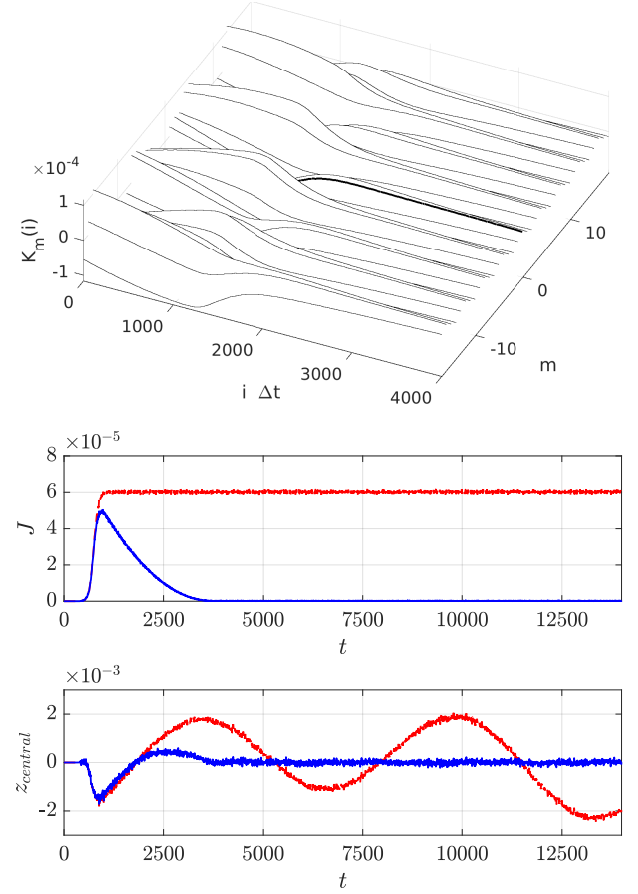


Fig. 5 Kernel function (top); cost function of the uncontrolled (red) and controlled (blue) cases (middle); central reference signal of the uncontrolled (red) and controlled (blue) cases (bottom).

function J is reduced by an order of magnitude as shown in Fig. 5. The converged kernel function shows strong dependency on the signal history up to 2000 time units, after which the history of the signal can be neglected, which is consistent with the assumption needed for switching the order of integration from eq. (3) to eq. (4). The frequency content of the signals in Fig. 6 shows that the control law generates an actuation signal with power in the spanwise frequency of interest as well, that is, the frequencies present in the upstream measurement y . Besides, the power spectral content (Fig. 7) of the reference signal z is reduced by roughly an order of magnitude, as expected from the behavior of the objective function J .

5 Conclusions

The study shows good performance of the studied control algorithm for the linearized Navier-Stokes equations, which means that as long as the behavior of the flow is well described by a linear model the control strategy will be able to dampen the disturbances. The fxLMS algorithm is capable of reconstructing the correct kernel function and achieve the desired reduction of the cost function as shown. The signal behavior is consistent with the flowfield behavior, meaning that such a set of sensors and actuators can capture the dynamics of the case. In conclusion, we have shown that the fxLMS control law is capable of dealing with such dynamics, that is, the advantages of an adaptive algorithm can be used for streaky disturbances as well.

6 Acknowledgements

We acknowledge the contribution of Shervin Bagheri and Nicolò Fabbiane (KTH) for helpful discussions. The authors acknowledge the funding from Vinnova through PreLaFloDes, Swedemo and CISB (Swedish-Brazilian Research and Innovation Centre). Simulations were performed at National Supercomputer Centre (NSC) and High Performance Computing Center North (HPC2N) with computational time provided by the Swedish National Infrastructure for Computing (SNIC).

References

- [1] N. Fabbiane. *Transition delay in boundary-layer flows via reactive control*. PhD thesis, KTH Mechanics, 2016.
- [2] N. Fabbiane, B. Simon, F. Fischer, S. Grundmann, S. Bagheri, and D. S. Henningson. *On the Role of Adaptivity for Robust Laminar-Flow Control*. J. Fluid Mech., 767:R1, 2015.
- [3] Sturzebecher, D. and Nitsche, W. (2003). *Active cancellation of Tollmien-Schlichting instabilities on a wing using multi-channel sensor actuator systems*. Intl J. Heat and Fluid Flow, 24, 572-583.

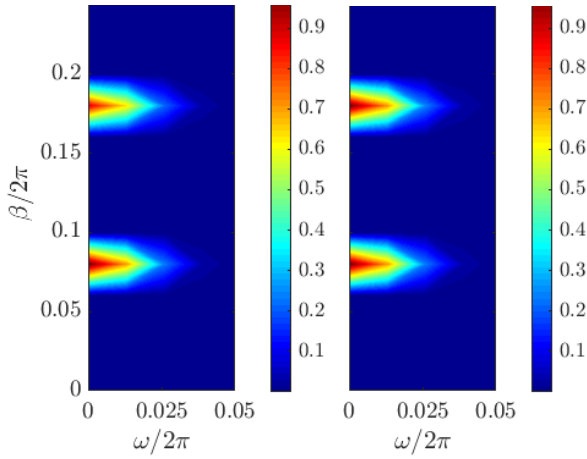


Fig. 6 Power spectrum of upstream measures y (left); Power spectrum of actuation signals u (right).

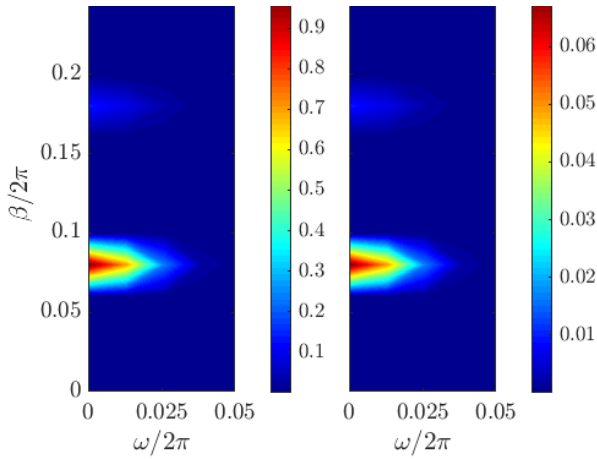


Fig. 7 Power spectrum of downstream measures z_d uncontrolled (left); power spectrum of downstream measure z_l controlled (right). Note the different magnitudes in the colorbars.

- [4] Kriegseis, J., Schwarz, C., Tropea, C., and Grundmann, S. (2013). *Velocity-Information-Based Force-Term Estimation of Dielectric-Barrier Discharge Plasma Actuators*. J. Phys. D, 46(5), 055202.
- [5] L. Brandt, P. Schlatter, and D. S. Henningson. *Transition in boundary layers subject to free-stream turbulence*. Journal of Fluid Mechanics, 517:167-198, 2004.
- [6] M. Chevalier, P. Schlatter, A. Lundbladh, and D. S. Henningson. *A pseudo-spectral solver for incompressible boundary layer flows*. Technical Report TRITA-MEK 2007:07, KTH Mechanics, Stockholm, Sweden, 2007.

7 Contact Author Email Address

P. Morra: pmorra@mech.kth.se

Copyright Statement

The authors confirm that they, and/or their company or organization, hold copyright on all of the original material included in this paper. The authors also confirm that they have obtained permission, from the copyright holder of any third party material included in this paper, to publish it as part of their paper. The authors confirm that they give permission, or have obtained permission from the copyright holder of this paper, for the publication and distribution of this paper as part of the ICAS proceedings or as individual off-prints from the proceedings.